The Journal of Neuroscience, June 15, 2001, 21(12):4259–4271

$p27^{Kip1}$ and $p57^{Kip2}$ Regulate Proliferation in Distinct Retinal Progenitor Cell Populations

Michael A. Dyer and Constance L. Cepko

Department of Genetics and Howard Hughes Medical Institute, Harvard Medical School, Boston, Massachusetts 02115

In the developing vertebrate retina, progenitor cell proliferation must be precisely regulated to ensure appropriate formation of the mature tissue. Cyclin kinase inhibitors have been implicated as important regulators of proliferation during development by blocking the activity of cyclin–cyclin-dependent kinase complexes. We have found that the $p27^{Kip1}$ cyclin kinase inhibitor regulates progenitor cell proliferation throughout retinal histogenesis. $p27^{Kip1}$ is upregulated during the late G_2/early G_1 phase of the cell cycle in retinal progenitor cells, where it interacts with the major retinal D-type cyclin–cyclin D1. Mice deficient for $p27^{Kip1}$ exhibited an increase in the proportion of mitotic cells throughout development as well as extensive apoptosis, particularly during the later stages of retinal histogenesis. Retroviral-mediated overexpression of $p27^{Kip1}$ in mitotic retinal progenitor cells led to premature cell cycle exit yet had no dramatic effects on Müller glial or bipolar cell fate specification as seen with the *Xenopus* cyclin kinase inhibitor, $p27^{Xic1}$. Consistent with the overexpression of $p27^{Kip1}$, mice lacking one or both alleles of $p27^{Kip1}$ maintained the same relative ratios of each major retinal cell type as their wild-type littermates. During the embryonic stages of development, when both $p27^{Kip1}$ and $p57^{Kip2}$ are expressed in retinal progenitor cells, they were found in distinct populations, demonstrating directly that different retinal progenitor cells are heterogeneous with respect to their expression of cell cycle regulators.

Key words: cyclin kinase inhibitor; apoptosis; cyclin D1; retrovirus; Müller glia; bipolar cell

The vertebrate retina is made up of six neuronal cell types and one glial cell type (for review, see Rodieck, 1998). In the murine retina, these diverse cell types are generated in a characteristic order during development (Young, 1985) from multipotent progenitor cells (Turner et al., 1990). It has been proposed that the birth order of retinal cell types reflects the unidirectional transition of progenitor cells through distinct stages of competence characterized by their ability to generate restricted subsets of retinal cell types (Cepko et al., 1996). Because of this developmental birth order, the proportion of cells that exit the cell cycle at each stage of development must be regulated carefully. If too many cells were to exit the cell cycle during the early stages of development, there might be an increase in the proportion of early-born cell types at the expense of later-born cell types.

In addition to the changes in progenitor competence over time during retinal histogenesis, there is evidence to suggest that at particular stages of development progenitors are a heterogeneous population that can exhibit biases in the fates adopted by their daughter cells (Alexiades and Cepko, 1997; Belliveau and Cepko, 1999; Belliveau et al., 2000). Therefore, along with the regulation of the total number of cells exiting the cell cycle over the course of retinal development, at any given stage of development the correct proportion of postmitotic daughter cells from each progenitor subpopulation also must be regulated carefully. If the newly postmitotic daughter cells were disproportionately derived from a subset of progenitor cells with a particular cell fate bias, then the proportion of cell types in the mature retina might be perturbed.

Previous research has demonstrated that the $p57^{Kip2}$ cyclin kinase inhibitor is upregulated in progenitor cells during the late G_1/G_0 phase of the cell cycle and mediates cell cycle exit in the murine retina (Dyer and Cepko, 2000a). However, $p57^{Kip2}$ is expressed in only a subset (~16%) of mitotic progenitors between embryonic day (E) 14.5 and 17.5, raising the intriguing possibility that progenitor cells may use different mechanisms to exit the cell cycle during development. Although it has been reported that $p27^{Kip1}$ is expressed in the embryonic retina (Zhang et al., 1998; Levine et al., 2000), a detailed analysis has not been performed on its role in the regulation of progenitor cell proliferation or cell fate specification. Moreover, it has not been established whether $p27^{Kip1}$ plays a semi-redundant role with $p57^{Kip2}$ in regulating progenitor cell proliferation or the two proteins function in distinct populations.

In the embryonic retina when both $p27^{Kip1}$ and $p57^{Kip2}$ are expressed, we have found that they are expressed in distinct progenitor cell populations and are upregulated at different times in the cell cycle. Loss of one or both alleles of $p27^{Kip1}$ was found to lead to extra rounds of cell division during development, but the distribution of the major cell types was not perturbed. In contrast to the $p57^{Kip2}$-deficient mice, apoptosis did not occur when cells reentered the cell cycle but came much later at the end of retinal histogenesis. Retroviral overexpression of $p27^{Kip1}$ in mitotic progenitor cells led to premature cell cycle exit, and as expected from premature exit, there was a reduction in the proportion of clones containing the cell types born at the end of retinal histogenesis: Müller glia and bipolar cells.

Received May 16, 2000; revised March 16, 2001; accepted March 20, 2001.

M.A.D. was supported by National Research Service Award fellowship EY06803-02 and the Charles H. Revson Foundation Fellowship for Biomedical Research. This work was supported by National Institutes of Health Grant EY0-8064. We thank Dr. M. H. Baron for many helpful discussions and support throughout this project; Drs. S. Elledge, W. Harper, P. Zhang, and W. Harris for cDNAs; Dr. L. H. Tsai for knock-out mice; M. Peters for critical reading of this manuscript; and J. Zitz, M. Peters, and L. Rose for technical support.

Correspondence should be addressed to Constance L. Cepko, Department of Genetics and Howard Hughes Medical Institute, Harvard Medical School, 200 Longwood Avenue, Boston, Massachusetts 02115. E-mail: cepko@rascal.med.harvard.edu.

MATERIALS AND METHODS

Animals. C57BL/6, CD1, and ICR mice were purchased from Taconic Farms (Germantown, NY). $p27^{Kip1}$ knock-out mice (Fero et al., 1996) were crossed to ICR or C57BL/6 mice with equivalent results. Genotypes were determined by performing PCR amplification of the wild-type and mutant alleles from tail DNA (Fero et al., 1996). Timed pregnant Sprague Dawley rats were purchased from Taconic Farms.

RNA isolation and RT-PCR assay. Three independent retinas were removed from staged embryonic (E14.5, E16.5, E18.5), postnatal (P0, P3, P6, P9, P12), and adult (6 weeks) ICR mice and immediately dissolved in 500 μl lysis solution (4 M guanidine thiocyanate, 25 mM sodium citrate, 0.5% Sarkosyl, 0.1 M β-mercaptoethanol). All three samples from each stage were analyzed, and a representative set is shown in Figure 1. RNA was prepared as described (Chomczynski and Sacchi, 1987). Expression of $p27^{Kip1}$, cyclin D1, cyclin D3, and β-actin was analyzed in each sample by performing semiquantitative RT-PCR as described previously (Farrington et al., 1997). Sequence for the β-actin primers can be found in Farrington et al. (1997). Oligonucleotide primers for mouse $p27^{Kip1}$ were (5′): 5′-AAACGTGAGAGTGTCTAACG-3′ (T_m = 51.4°C) and (3′): 5′-CCGTCTGAAACATTTTCTT-3′ (T_m = 51.2°C). Oligonucleotide primers for mouse cyclin D1 were (5′): 5′-ATGGAACACCAGCTCCTG-3′ (T_m = 55.3°C) and (3′):5′-CCAGACCAGCCTCTTCC-3′ (T_m = 54.5°C). Oligonucleotide primers for mouse cyclin D3 were (5′): 5′-TGTCCTGCAGAGTTTACTCC-3′ (T_m = 53.9°C) and (3′): 5′-GCAGGCAGTCCACTTCA-3′ (T_m = 54.9°C).

Immunohistochemistry, microscopy, and imaging. Retinal cryosections or dissociated cells (see below) were fixed in paraformaldehyde (4% in PBS), washed, and treated with hydrogen peroxide (1% in PBS) before incubation in blocking solution [PBS containing 0.1% Triton X-100 and 2% normal serum (Vector Laboratories, Burlingame, CA)]. For each of the antibodies listed below, the dilution used for retinal sections is listed first, followed by the dilution used for dissociated cell staining where applicable. Normal donkey serum was used for the following antibodies: anti-$p27^{Kip1}$, clone 57 (mouse monoclonal, 1:50, 1:2000; Transduction Labs); anti-rhodopsin, Rho4D2 [mouse monoclonal, 1:250, 1:2000 (Molday and MacKenzie, 1983)]; anti-calretinin (mouse monoclonal, 1:500, 1:2000; Chemicon, Temecula, CA); anti-HNK-1, VC1.1 (mouse monoclonal, 1:1000, 1:5000; Sigma, St. Louis, MO); anti-syntaxin, HPC-1 (mouse monoclonal, 1:1000, 1:5000; Sigma); anti-calbindin-D28K, CL-300 (mouse monoclonal, 1:200, 1:2000; Sigma); anti-cyclin D1, 72–13G (mouse monoclonal, 1:500; Santa Cruz Biotechnology, Santa Cruz, CA); anti-FLAG, M2 (mouse monoclonal, 1:100; Sigma); and anti-bipolar antigen, 115A10 [mouse monoclonal, undiluted(Onoda and Fujita, 1987)] antibodies. Normal goat serum was used for the anti-cyclin D3 (rabbit polyclonal, 1:200; Santa Cruz Biotechnology); anti-choline aceltyltransferase (rabbit polyclonal, 1:400, 1:2000; Chemicon); anti-Chx10 [rabbit polyclonal, 1:1000, 1:5000 (C. Cepko, unpublished data)[; anti-cellular retinaldehyde binding protein (CRALBP) [rabbit polyclonal, 1:1000, 1:5000 (De Leeuw et al., 1990)]; and anti-cone opsins [rabbit polyclonal, 1:5000 (Wang et al., 1992; Chiu et al., 1994)] antibodies. Normal rabbit serum was used for the anti-$p57^{Kip2}$, E-17 (goat polyclonal, 1:50, Santa Cruz Biotechnology) antibody. Biotin-conjugated secondary antibodies (donkey anti-mouse IgG, rabbit anti-goat IgG, goat anti-rabbit IgG; Vector Laboratories) were used at a dilution of 1:500 in blocking solution. After secondary antibody binding, an avidin–biotin–peroxidase complex (Vectastain ABC, Vector Laboratories) was incubated with the sections or dissociated cells followed by diaminobenzidine detection (Vector Laboratories), FITC tyramide, or Cy-3 tyramide detection (DuPont NEN, Wilmington, DE) according to the manufacturers' instructions (Bobrow et al., 1991). For some experiments, flurophor-conjugated tyramine compounds and reaction buffers were synthesized according to previous reports (Bobrow et al., 1991) with equivalent results. For nuclear staining, DAPI was added to the final wash solution at 0.0005%. Labeled cells were visualized using a Zeiss Axioplan-2 microscope with 10×, 20×, and 40× Plan Neofluar objectives or a 100× Plan Apochromat objective with adjustable iris. Images were captured with a Spot digital camera (Diagnostic Instruments). Confocal microscopy was performed using a Leica DM-RBE microscope equipped with a TCSNT true confocal scanner.

[^{3}H] thymidine and BrdU labeling. To label retinal progenitor cells in S-phase, retinas were incubated in 1 ml explant culture medium containing [^{3}H] thymidine [DuPont NEN; 5 μCi/ml (89 Ci/mmol)] or 10 μM bromodeoxyuridine (BrdU) (Boehringer Mannheim, Indianapolis, IN) for 1 hr at 37°C. Autoradiography and BrdU detection were performed as described previously (Morrow et al., 1998).

Retinal explant culture and dissociation. The procedure for explant culturing of mouse retinas has been described in detail previously (Dyer and Cepko, 2000a). Extensive characterization has demonstrated that retinal proliferation and differentiation are normal using this explant culture system (Dyer and Cepko, 2000a). Tissue dissociation was performed as described previously (Morrow et al., 1998).

Replication incompetent retroviral vector constructs and viral production. Oligonucleotides encoding the FLAG–His cassette were synthesized [for sequence, see Dyer and Cepko (2000a)], annealed, and cloned into the pNIN replication incompetent retroviral vector (Cepko, unpublished data) to make pNIN-E, the pLIA replication incompetent retroviral vector (Cepko et al., 1998) to make pLIA-E, or the pGFP vector to make pGFP-E. Mouse $p27^{Kip1}$ was PCR amplified, sequenced, and cloned into pNIN-E, pLIA-E, and pGFP-E to generate pNIN-E^{p27}, pLIA-E^{p27}, and pGFP-E^{p27}, respectively. Oligonucleotide primers for $p27^{Kip1}$ PCR amplification were as follows: p27-amino, 5′-TAGAGCGGCCGCATCTAACGTGAGAGTGTCT-3′ and p27-carboxy, 5′-TAGAGCGGCCGCCGTCTGGCGTCGAAGGCC-3′.

Xenopus $p27^{Xic1}$ was PCR amplified, sequenced, and cloned into pLIA-E to generate pLIA-E^{Xic1}. Oligonucleotide primers for $p27^{Xic1}$ were as follows: Xic1-amino, 5′-TAGAGCGGCCGCAGCTGCTTTDCCACATCGCC-3′ and Xic1-carboxy, 5′-TAGAGCGGCCGCTCGAATCTTTTTCCTGGG-3′.

To prepare high-titer retroviral stocks, the plasmid constructs were transiently transfected into a 293T ecotropic producer cell line (Phoenix-E) by calcium phosphate coprecipitation as described (Cepko et al., 1998). Supernatant containing the viral particles was harvested at 48 hr after transfection, and viral titer was determined on NIH-3T3 cells (Cepko et al., 1998). *In vivo* lineage analysis was performed as described previously (Turner and Cepko, 1987; Fields-Berry et al., 1992).

Recombinant $p27^{Kip1}$ purification, coimmunoprecipitation, and immunoblotting. Recombinant histidine-tagged $p27^{Kip1}$ was prepared using a baculovirus expression vector system (PharMingen, San Diego, CA) and purified on Ni^{2+}-NTA agarose resin (Qiagen, Hilden, Germany) according to the manufacturer's instructions for nondenaturing conditions (Dyer and Cepko, 2000a). Recombinant proteins were used as positive controls for immunoprecipitation and immunoblotting experiments. For cyclin D1 coimmunoprecipitation, 10 P0 retinas from CD1 mouse pups were sonicated briefly in 2 ml 1× RIPA buffer (1× PBS, 1% NP-40, 0.5% sodium deoxycholate, 0.1% SDS, 1 mM PMSF) containing a cocktail of protease inhibitors (Sigma), and phosphatase inhibitors (1 mM Levamisole, 2 mM Na_2VO_3, 1 mM NaF). This crude retinal lysate was cleared by spinning at 14,000 × *g* and protein-G Agarose preclearing was performed according to the manufacture's instructions (Santa Cruz Biotechnology). Anti-cyclin D1, C-20 (rabbit polyclonal, 1 μg; Santa Cruz Biotechnology) antibody was incubated with gentle inversion for 1 hr followed by a 1–2 hr incubation with protein-G Agarose. Washes and elution were performed according to the manufacturer's instructions (Santa Cruz Biotechnology). Crude retinal lysates, washes, and immunoprecipitates were separated on a 12% polyacrylamide gel containing SDS and transferred to nitrocellulose. Blocking, washing, and primary antibody incubations (anti-$p27^{Kip1}$, 1:1000) were performed according to the manufacturer's instructions (Transduction Labs). The secondary biotinylated antibody (donkey anti-mouse IgG; Vector Laboratories) was used at a dilution of 1:2000. Amplification was achieved by incubating the immunoblot with an avidin–biotin–alkaline phosphatase complex (Vectastain-AP, Vector Laboratories) followed by nitro blue tetrazolium–5-bromo-4-chloro-3-indolyl phosphate detection (Vector Laboratories).

Apoptosis analysis. The colorimetric apoptosis detection system [terminal deoxynucleotidyl transferase-mediated biotinylated dUTP nick end labeling (TUNEL)] was used on 20 μm cryosections according to the manufacturer's instructions (Promega, Madison, WI).

Dissociated cell scoring and statistical methods. To evaluate the significance of differences in the proportion of cell types between wild-type, $p27^{Kip1}$-heterozygous, and $p27^{Kip1}$-deficient retinas, the mean and SD were calculated for counts of retinas from each genotype, and a *t* test was performed. All *p* values are one-sided unless indicated otherwise.

RESULTS

$p27^{Kip1}$ expression during development

As a first step toward understanding the kinetics of $p27^{Kip1}$ mRNA expression over the course of retinal histogenesis, semiquantitative RT-PCR analysis was performed on three indepen-

dent retinas from eight stages of development. Using primers specific for the $p27^{Kip1}$ coding sequence, mRNA was detected at E14.5 and persisted throughout development, peaking around P0 when the number of mitotic cells producing postmitotic daughter cells is the highest in the rodent retina (Fig. 1*A*) (Alexiades and Cepko, 1996). Notably, $p27^{Kip1}$ expression was also found in the adult retina where there are no mitotic cells present (Fig. 1*A*). For comparison, oligonucleotide primers specific for transcripts from the cyclin D1 and D3 genes were included in this analysis. It has been well established that cyclin D1 is the major D-type cyclin found in mitotic retinal progenitor cells during development (Fantl et al., 1995; Sicinski et al., 1995), and cyclin D3 is expressed in Müller glial cells of adult retina (Dyer and Cepko, 2000b; C. Ma and C. Cepko, unpublished observations). Because the percentage of mitotic cells decreased during development (Alexiades and Cepko, 1996), cyclin D1 mRNA expression tapered off such that in the mature retina, very little cyclin D1 was detected (Fig. 1*A*). In contrast to cyclin D1, cyclin D3 was expressed at very low levels in the developing retina but was sharply upregulated during the late perinatal stages (Fig. 1*A*).

The cellular distribution of the $p27^{Kip1}$ protein was examined by performing immunohistochemical staining on mouse retinas from six stages of development (Fig. 1*C–F*) (data not shown). An antibody specific for cyclin D1 was included to label the mitotic retinal progenitor cells (Fig. 1*B*,*G*) (data not shown). Cells move within the developing retina according to cell cycle phase; mitosis occurs adjacent to the pigmented epithelium (PE), and S-phase occurs closer to the vitreal surface near the boundary between the inner neuroblastic layer (inbl) and the outer neuroblastic layer (onbl) (Sauer, 1937). The two gap phases (G_1 and G_2) mark the movement of cells between the PE and the inbl/onbl boundary. At E14.5, two populations of $p27^{Kip1}$-expressing cells were detected (Fig. 1*C*). A subset of cells along the outer edge of the retina where newly postmitotic neurons fated to be cones and rods are found, as well as those on the inner surface where ganglion cells are differentiating, expressed high levels of $p27^{Kip1}$ (Fig. 1*C*). A second group of $p27^{Kip1}$-immunoreactive cells was detected throughout the onbl in the region where cyclin D1 is normally expressed (Fig. 1, compare *B*, *C*).

At later stages of development (Fig. 1*D–F*), $p27^{Kip1}$ was also expressed in gap phase cells along with newly postmitotic cells in the developing inner nuclear layer (INL) and ganglion cell layer (GCL). Cyclin D1 was expressed primarily in mitotic cells and appeared to be downregulated quickly in these newly postmitotic daughter cells (Fig. 1*G*) (data not shown). In the adult retina, $p27^{Kip1}$ expression colocalized with cyclin D3 in Müller glial cells (Dyer and Cepko, 2000b).

Previous work has demonstrated that a subset of progenitor cells exiting the cell cycle in the embryonic retina upregulate $p57^{Kip2}$ (Dyer and Cepko, 2000a). To determine whether $p27^{Kip1}$ and $p57^{Kip2}$ are found in distinct progenitor cell populations, double-label immunocytochemical staining was performed on E14.5 retinal sections with antibodies directed against $p27^{Kip1}$ and $p57^{Kip2}$. We found that these two proteins did not colocalize in the E14.5 retina (Fig. 1*H–J*). Similarly, in the adult retina (Fig. 1*K–M*), these two proteins defined distinct, highly restricted populations of retinal neurons and glia (Dyer and Cepko, 2000b; Dyer and Cepko, 2001).

Timing of $p27^{Kip1}$ upregulation during the cell cycle

To determine whether the onset of $p27^{Kip1}$ expression within the cell cycle indicates that it might regulate progenitor cell proliferation, the expression of $p27^{Kip1}$ was examined during different phases of the cell cycle. S-phase cells were pulse-labeled by incubating retinas with [^{3}H]thymidine for 1 hr. After [^{3}H]thymidine labeling, retinas were cultured as explants for various lengths of time, dissociated, and reacted with antisera specific for $p27^{Kip1}$. After autoradiography, the proportion of [^{3}H]thymidine-labeled cells expressing $p27^{Kip1}$ was scored (Fig. 2*A–C*, Table 1). This analysis was performed at four stages of development (E14.5, E17.5, P0, and P2), spanning the period when $p27^{Kip1}$ is expressed in retinal progenitor cells (Fig. 2*D–G*, Table 1). It was critical to examine all of these stages because the proliferation properties of retinal progenitor cells change during development in rodents (Alexiades and Cepko, 1996), and we wanted to determine whether the onset of $p27^{Kip1}$ expression during the cell cycle reflected those changes.

At E14.5, immediately after labeling ($t = 0$), none of the cells expressing $p27^{Kip1}$ (0/270, 0%) were labeled with [^{3}H]thymidine and therefore were not in S-phase (Fig. 2*D*, Table 1). Four hours later ($t = 4$), when many of the [^{3}H]thymidine-labeled cells would have entered G_2 (Alexiades and Cepko, 1996), some (27/328, 8.2%) [^{3}H]thymidine-labeled cells expressed $p27^{Kip1}$ (Fig. 2*D*, Table 1). Progenitors in S-phase at the time of labeling should begin to enter G_1 by 8 hr ($t = 8$) after labeling (Alexiades and Cepko, 1996). At that time point, a significant increase (57/361, 15.8%) in the proportion of [^{3}H]thymidine-labeled cells expressing $p27^{Kip1}$ was observed (Fig. 2*D*, Table 1). Later time points showed a slight increase in the proportion of double-labeled cells (Fig. 2*D*, Table 1); however, the vast majority of retinal progenitor cells upregulated $p27^{Kip1}$ during the late portion of G_2 or early part of G_1, consistent with the $p27^{Kip1}$ expression pattern seen at E14.5 (Fig. 1). Transcription is silenced during M phase so it is unlikely that $p27^{Kip1}$ is upregulated during this phase of the cell cycle (Sanchez and Dynlacht, 1996).

From the earliest stages of retinal development in rodents when the first postmitotic daughter cells are being generated to the cessation of mitotic activity, the length of the cell cycle increases from ~14 hr at E14.5 to ~55 hr at P8 (Alexiades and Cepko, 1996). The timing of $p27^{Kip1}$ upregulation in individual progenitor cells during the cell cycle may reflect this change in cell cycle kinetics, or cell cycle length may be intrinsically regulated. To distinguish between these two possibilities, a similar [^{3}H]thymidine-labeling experiment was performed at E17.5, P0, and P2 (Fig. 2*E–G*, Table 1). By E17.5 the timing of the onset of $p27^{Kip1}$ expression was delayed by ~4 hr as compared with the E14.5 labeling experiment (Fig. 2*E*, Table 1), and in postnatal retinal progenitor cells (P0, P2) there was an even longer delay (14 hr) in the accumulation of [^{3}H]thymidine-labeled cells expressing $p27^{Kip1}$ (Fig. 2*F*,*G*, Table 1).

Cyclin D1 is the major D-type cyclin found in mitotic retinal progenitor cells of the murine retina and is required for progenitor cell proliferation (Fantl et al., 1995; Sicinski et al., 1995; Ma et al., 1998). Because of this central role in regulating retinal progenitor cell proliferation, a coimmunoprecipitation experiment was performed to determine whether $p27^{Kip1}$ interacts with cyclin D1 *in vivo*. Protein lysates from P0 retinas were incubated with an anti-cyclin D1 antibody, immunoprecipitated, separated by SDS-PAGE, and immunoblotted with an antibody specific for $p27^{Kip1}$. Cyclin D1 and $p27^{Kip1}$ formed a complex in lysates from retinas when the number of mitotic cells was highest (Alexiades and Cepko, 1996) (Fig. 2*H*).

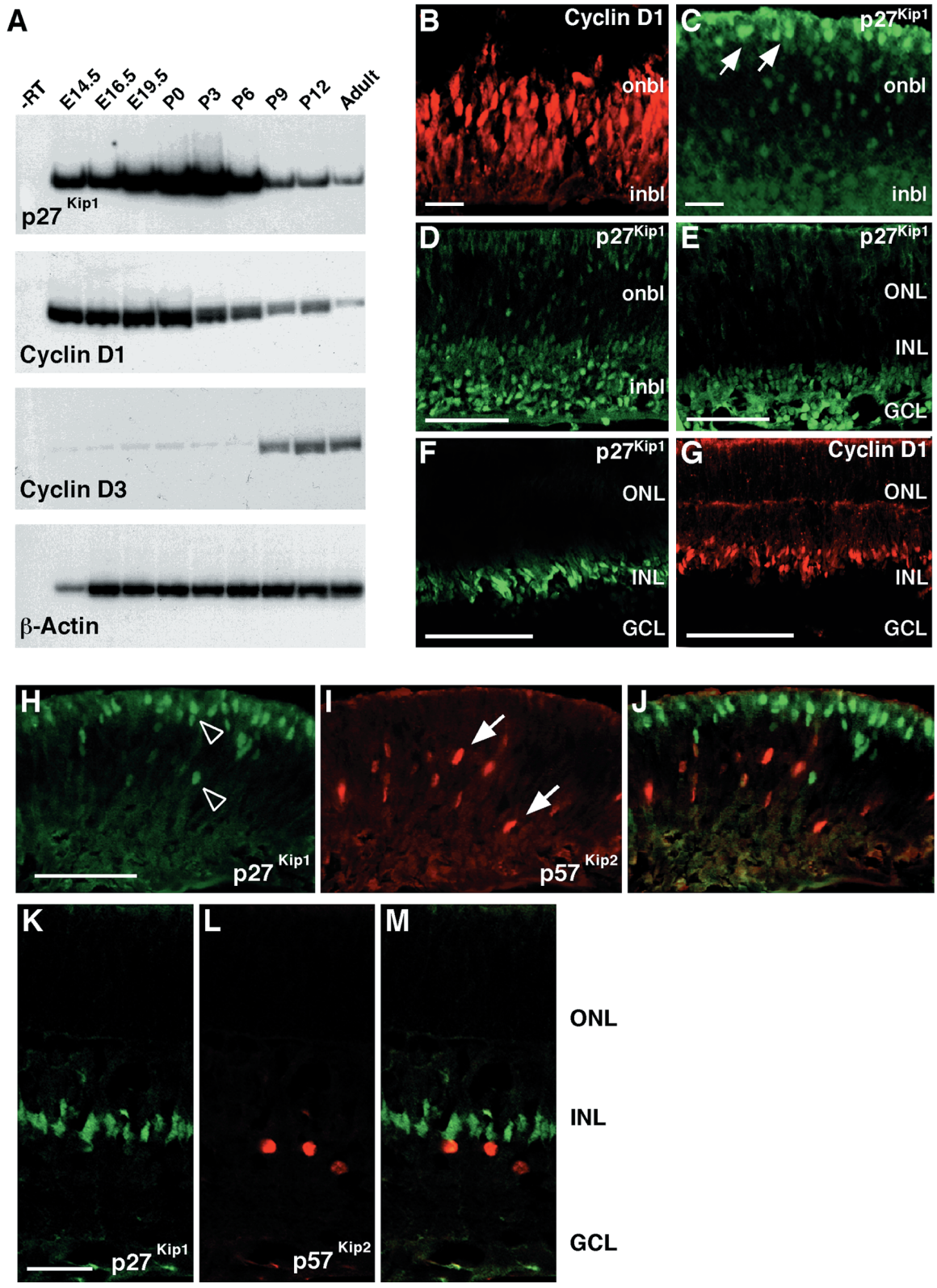

Figure 1. $p27^{Kip1}$ expression during retinal development. *A–G*, The temporal expression and distribution of cyclin D1, D3, and $p27^{Kip1}$ mRNA and protein was examined by semiquantitative RT-PCR (*A*) and immunohistochemistry (*B–G*). *A*, Representative RT-PCR reactions are shown for each stage examined using primers specific for $p27^{Kip1}$, cyclin D1, and cyclin D3. β-actin served as an internal control for the efficiency of RNA isolation and cDNA synthesis. *B*, Cyclin D1 protein was broadly expressed in progenitor cells occupying the outer neuroblastic layer (*onbl*) at E14.5 in the mouse retina. *C*, $p27^{Kip1}$ protein was expressed strongly in the inner neuroblastic layer (*inbl*), which is occupied by cells that have recently exited the cell cycle, as well as along the outer edge of the retina adjacent to the developing pigmented epithelium (*arrows*). In addition, weaker expression was observed in the onbl where cyclin D1 is expressed. *D–F*, Throughout development, embryonic day 17.5 (*D*), postnatal day 3 (*E*), and postnatal day 6 (*F*), $p27^{Kip1}$ was expressed in newly postmitotic cells and to a lesser extent in the regions where mitotic progenitor cells expressing cyclin D1 (*Figure legend continues*.)

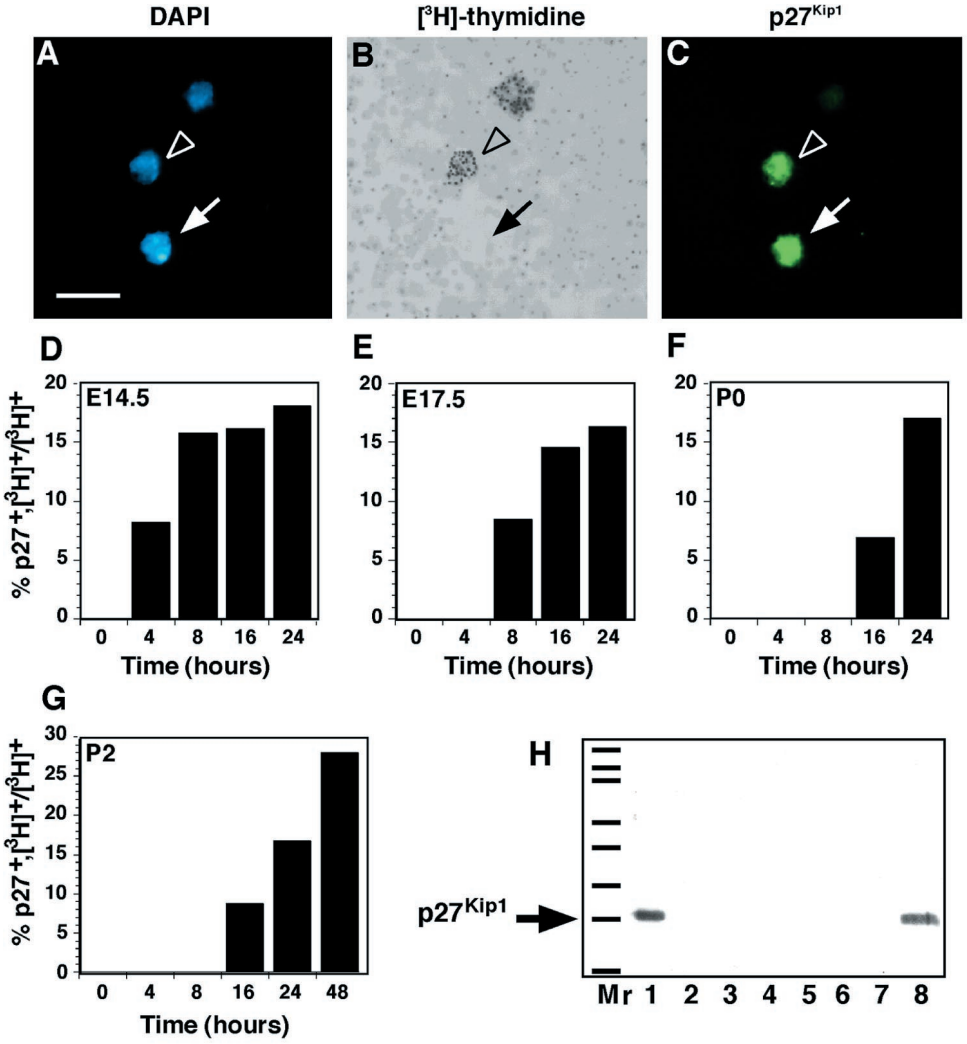

Figure 2. Expression of $p27^{Kip1}$ in retinal progenitor cells during the cell cycle. Immunofluorescent and autoradiographic analyses were performed on dissociated cells from retinas at E14.5, E17.5, P0, and P2 incubated with [^{3}H]thymidine for 1 hr. *A–C*, A representative field of E14.5 cells showing a cell that was in S-phase at the time of labeling that upregulated $p27^{Kip1}$ after 8 hr in culture (*open arrowheads*) and a $p27^{Kip1}$-immunoreactive cell that was not in S-phase at the time of labeling (*closed arrows*). *D–G*, Histograms of the proportion of [^{3}H]thymidine-positive cells that are $p27^{Kip1}$ immunopositive at the indicated time points for each stage of development (Table 1). *H*, Anti-$p27^{Kip1}$ immunoblot of anti-cyclin D1 immunoprecipitate. Lanes are as follows: *1*, starting crude lysate; *2*, supernatant after immunoprecipitation; *3–6*,each of four successive washes of the immunoprecipitate; 7, control IgG immunoprecipitation; and *8*, anti-cyclin D1 immunoprecipitation. M_r protein markers, relative molecular mass from bottom: 20, 26, 36, 42, 66, 97, 116, 158 kDa.

Retroviral-mediated overexpression of $p27^{Kip1}$ in mitotic retinal progenitor cells

To test whether $p27^{Kip1}$ expression is sufficient to drive retinal progenitor cells out of the cell cycle, and to examine any effects of $p27^{Kip1}$ overexpression on cell fate specification, three replication incompetent retroviruses containing the $p27^{Kip1}$ cDNA were generated (Fig. 3*A*). One of these viral constructs (Fig. 3*A*, *pNIN-E$^{(Kip1)}$*) contains a nuclear β-galactosidase reporter gene and is ideally suited for analyzing the effects of $p27^{Kip1}$ overexpression on progenitor cell proliferation (Dyer and Cepko, 2000a). The second viral construct (Fig. 3*A*, *pLIA-E$^{(Kip1)}$*) contains an alkaline phosphatase reporter gene and is similar to constructs used previously for *in vivo* lineage analysis in the rodent retina (Cepko et al., 1998). A retroviral construct encoding green fluorescent protein (GFP) was also generated for co-immunolocalization experiments. By taking advantage of the epitope tag (FLAG) encoded on the amino terminus of $p27^{Kip1}$ in these vectors (Fig. 3*A*), we demonstrated that significant levels of $p27^{Kip1}$ protein were expressed from pNIN-E^{Kip1} and pLIA-E^{Kip1} (Fig. 3*B*). Furthermore, infected fibroblasts (NIH-3T3) exited the cell cycle but did not undergo apoptosis (data not shown). Finally, immunolocalization of the FLAG epitope in 293T cells transfected with a similar retroviral construct encoding GFP (Fig. 3*A*, *pGFP-E$^{(Kip1)}$*) demonstrated that most cells (189/200, 94%) expressing GFP also express nuclear-localized $p27^{Kip1}$ (Fig. 3*C*).

To examine the effects of $p27^{Kip1}$ overexpression on progenitor cell proliferation, E14.5 murine retinas (n = 43) were infected with NIN-E^{Kip1} or NIN-E and cultured for 10 d as explants (see Materials and Methods). After this culture period, retinas were

←

can be found at postnatal day 6 (*G*) and postnatal day 3 (data not shown). *H–M*, Immunolocalization of $p27^{Kip1}$ and $p57^{Kip2}$ in the embryonic (*H–J*) and adult (*K–M*) retina. Two distinct progenitor populations were detected at E14.5; one group expressed $p27^{Kip1}$ (*green* fluorescence) (*H*), and the other expressed $p57^{Kip2}$ (*red* fluorescence) (*I*). *J*, *Green* and *red* fluorescence were overlaid to demonstrate that these two proteins are found in distinct populations of embryonic retinal cells. *K–M*, Immunolocalization of $p27^{Kip1}$ and $p57^{Kip2}$ in the adult retina. Müller glial cells express $p27^{Kip1}$ (*green* fluorescence) (*K*), and a subpopulation of amacrine cells express $p57^{Kip2}$ (*red* fluorescence) (*L*) in the adult retina. *M*, *Green* and *red* fluorescence were layered to demonstrate that these two proteins are found in distinct populations of cells in the mature retina. *Open arrowheads* indicate $p27^{Kip1}$-immunoreactive nuclei, and *closed arrows* indicate representative $p57^{Kip2}$-immunoreactive nuclei. *inbl*, Inner neuroblastic layer; *onbl*, outer neuroblastic layer; *ONL*, outer nuclear layer; *INL*, inner nuclear layer; *GCL*, ganglion cell layer; *-RT*, -reverse transcriptase. Scale bars: *B*, *C*, *H–J*, 20 μm; *D–G*, 100 μm; *H–M*, 50 μm.

Table 1. $p27^{Kip1}$ is upregulated during the late G_2/early G_1 phase of the cell cycle during development

Stage	Culture time[a] (hr)	[^{3}H]thy$^+$/total (counts; mean % ± SD)[b]	$p27^{Kip1+}$/total (counts; mean % ± SD)	$p27^{Kip1+}$, [^{3}H]thy$^+$/[^{3}H]thy$^+$ (counts, %)
E14.5	0	124/500, 147/500 (27 ± 3.2)	252/500, 274/500 (53 ± 3.1)	0/270, 0
E14.5	4	171/500, 157/500 (33 ± 2.0)	211/500, 248/500 (46 ± 5.2)	27/328, 8.2
E14.5	8	179/500, 182/500 (36 ± 0.4)	204/500, 267/500 (47 ± 8.9)	57/361, 15.8
E14.5	18	264/500, 222/500 (48.6 ± 6.0)	262/500, 263/500 (48 ± 5.5)	79/486, 16.2
E14.5	24	291/500, 279/500 (57 ± 1.7)	242/500, 267/500 (51 ± 3.8)	103/570, 18.1
E17.5	0	117/500, 108/500 (22 ± 1.3)	231/500, 213/500 (44 ± 0.2)	0/225, 0
E17.5	4	114/500, 140/500 (25 ± 3.7)	211/500, 266/500 (48 ± 7.7)	0/254, 0
E17.5	8	130/500, 134/500 (26 ± 0.5)	250/500, 268/500 (52 ± 2.5)	23/270, 8.5
E17.5	18	183/500, 193/500 (38 ± 1.4)	238/500, 219/500 (49 ± 2.7)	35/376, 14.6
E17.5	24	197/500, 201/500 (40 ± 0.5)	264/500, 245/500 (51 ± 2.2)	81/498, 16.3
P0	0	69/500, 87/500 16 ± 2.5	338/500, 280/500 (62 ± 8.2)	0/156, 0
P0	4	106/500, 90/500 20 ± 2.2	236/500, 287/500 (52 ± 7.2)	0/196, 0
P0	8	83/500, 99/500 18 ± 2.2	298/500, 288/500 (59 ± 1.4)	0/182, 0
P0	18	97/500, 105/500 (20 ± 1.1)	264/500, 271/500 (53 ± 1.0)	14/202, 6.9
P0	24	120/500, 112/500 (23 ± 1.1)	278/500, 257/500 (54 ± 2.7)	40/232, 17
P2	0	22/500, 29/500 (5.1 ± 1.0)	249/500, 261/500 (51 ± 1.7)	0/51, 0
P2	4	45/500, 34/500 (7.9 ± 1.5)	347/500, 298/500 (64 ± 6.9)	0/79, 0
P2	8	38/500, 47/500 (8.5 ± 1.2)	339/500, 284/500 (62 ± 7.7)	0/85, 0
P2	18	96/500, 84/500 (18 ± 1.7)	288/500, 262/500 (55 ± 3.7)	16/180, 8.8
P2	24	110/500, 122/500 (23 ± 1.7)	250/500, 244/500 (49 ± 0.8)	39/232, 16.8
P2	48	78/500, 131/500 (21 ± 7.4)	288/500, 261/500 (55 ± 3.5)	60/209, 28

[a]Freshly dissected retinae (three to six) were incubated with [^{3}H]thymidine in culture medium for 1 hr, washed, and cultured as explants for the amount of time indicated.
[b]The number of grains for 10 randomly selected [^{3}H]thymidine-labeled cells varied from 20 to 67 grains per cell (mean = 48 ± 16). The number of grains for 14 randomly selected unlabeled cells varied from zero to six grains per cell (mean = 2.0 ± 1.6).

stained for β-galactosidase expression and sectioned, and the size of clones derived from single infected progenitor cells was scored (Fig. 3*D–F*). A distribution in clone size ranging from 1 to 29 cells was observed in retinas infected with the control virus (NIN-E) and from 1 to 16 cells for the retinas infected with NIN-E^{Kip1} (Fig. 3*F*). The proportion of single cell clones in retinas infected with NIN-E^{Kip1} (51/102, 50 ± 2.7%) was significantly increased compared with those infected with the control virus (50/160, 30 ± 2.2%) ($p < 0.01$) (Fig. 3*F*). Furthermore, the proportion of large clones (more than five cells) was significantly higher in retinas infected with NIN-E (50/160, 33 ± 2.4%) than NIN-E^{Kip1} (13/102, 13 ± 0.3%) ($p < 0.003$) (Fig. 3*F*).

Although these data suggest that overexpression of $p27^{Kip1}$ may be sufficient to drive retinal progenitor cells out of the cell cycle, it is possible that the smaller clone size resulted from apoptosis as a consequence of $p27^{Kip1}$ overexpression. Therefore we compared the kinetics of clone size distribution in retinas infected with NIN-E with those infected with NIN-E^{Kip1} over the course of several days in culture (Fig. 3*G*). If apoptosis played a significant role in the reduction of the size of clones derived from progenitor cells infected with NIN-E^{Kip1}, there might be an early peak in clone size followed by a decrease attributable to apoptosis. Alternately, if $p27^{Kip1}$ overexpression simply forced progenitor cells out of the cell cycle, then the decrease in clone

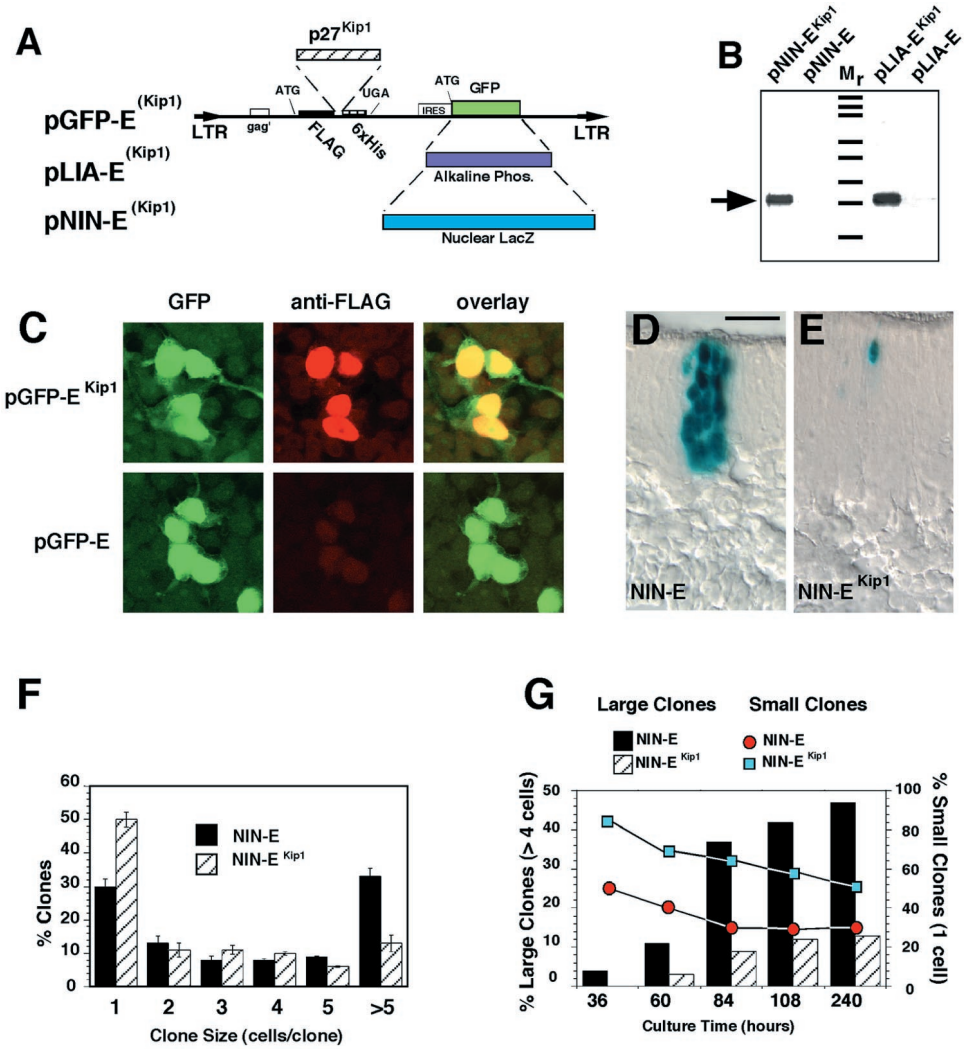

Figure 3. Overexpression of $p27^{Kip1}$ in embryonic mitotic retinal progenitor cells. *A*, Mouse $p27^{Kip1}$ was overexpressed using one of the three replication incompetent retroviral vectors shown. These constructs contain the mouse $p27^{Kip1}$ cDNA flanked by an epitope (*FLAG*) and purification (*6xHis*) tag. The bicistronic mRNA produced from these viruses or plasmids encodes $p27^{Kip1}$ and alkaline phosphatase for *in vivo* lineage analysis (LIA-E^{Kip1}), nuclear localized β-galactosidase for quantitation of clone size (NIN-E^{Kip1}), or green fluorescent protein (GFP-E^{Kip1}) for coimmunolocalization studies. *B*, An anti-FLAG immunoblot of Ni^{2+}-NTA Agarose purified eluate from NIH-3T3 cells infected with the indicated viral stocks. The *arrow* indicates $p27^{Kip1}$. *C*, 293T cells transfected with pGFP-E^{Kip1} express both GFP and nuclear localized $p27^{Kip1}$ (*red* fluorescence) as measured using an anti-FLAG antibody. Cells transfected with pGFP-E exhibit no FLAG immunoreactivity. *D*, *E*, Clone size can be readily scored (18 cells and 1 cell, respectively) in embryonic retinas infected with NIN-E^{Kip1} or its derivatives on sections stained for β-galactosidase expression. *F*, Between 100 and 200 clones for each virus were scored from two independent experiments to obtain the clone size distribution data. *G*, Approximately 600 clones were scored to obtain the kinetics of clone growth after infection with pNIN-E or pNIN-E^{Kip1}. *Bars* represent the accumulation of larger clones (>4 cells), whereas *circles* and *squares* represent the number of one-cell clones during the same culture period. The minimum amount of time required for histochemically detectable expression from these vectors in retinal progenitor cells is 36 hr. *LTR*, Long terminal repeat; *IRES*, internal ribosome entry site; *GFP*, green fluorescent protein; *ATG*, start codon; *UGA*, stop codon; *gag'*, truncated retroviral gag gene; M_r, protein markers, relative molecular mass from bottom: 20, 26, 36, 42, 66, 97, 116, 158 kDa. Scale bar, 20 μm.

size should remain relatively constant over the culture period. Data from >600 clones suggest that large clones are not generated and then pruned by apoptosis to reduce the clone size resulting from progenitor cells overexpressing $p27^{Kip1}$ (Fig. 3*G*). As additional support for this conclusion, no increase in the proportion of apoptotic nuclei was detected in clones ($n > 50$) expressing $p27^{Kip1}$ using the TUNEL assay (data not shown).

In the *Xenopus* retina, transfection of progenitor cells with a plasmid encoding $p27^{Xic1}$ led to an increase in the number of Müller glial cells at the expense of bipolar neurons (Ohnuma et al., 1999). To test whether $p27^{Xic1}$ could induce a similar alteration in cell fate specification in the rodent retina, a high titer stock of the LIA-E^{Xic1} retrovirus was injected into the left eye of newborn rat pups; the control LIA-E virus was injected into the contralateral eye (Cepko et al., 1998). Retinas were harvested after complete retinal development (P21), stained for alkaline phosphatase expression, and sectioned. Clones of cells derived from individually infected retinal progenitor cells (Fig. 4*A–F*) were scored for clone size and clone composition (Fig. 4*G*,*H*) (Turner and Cepko, 1987; Fields-Berry et al., 1992). Similar to the data from *Xenopus* (Ohnuma et al., 1999), the proportion of clones containing bipolar interneurons was decreased from 19% (32/165) for LIA-E to 8% (35/416) for LIA-E^{Xic1} (Fig. 4*G*). If all of the infected cells are treated as a population, then the propor-

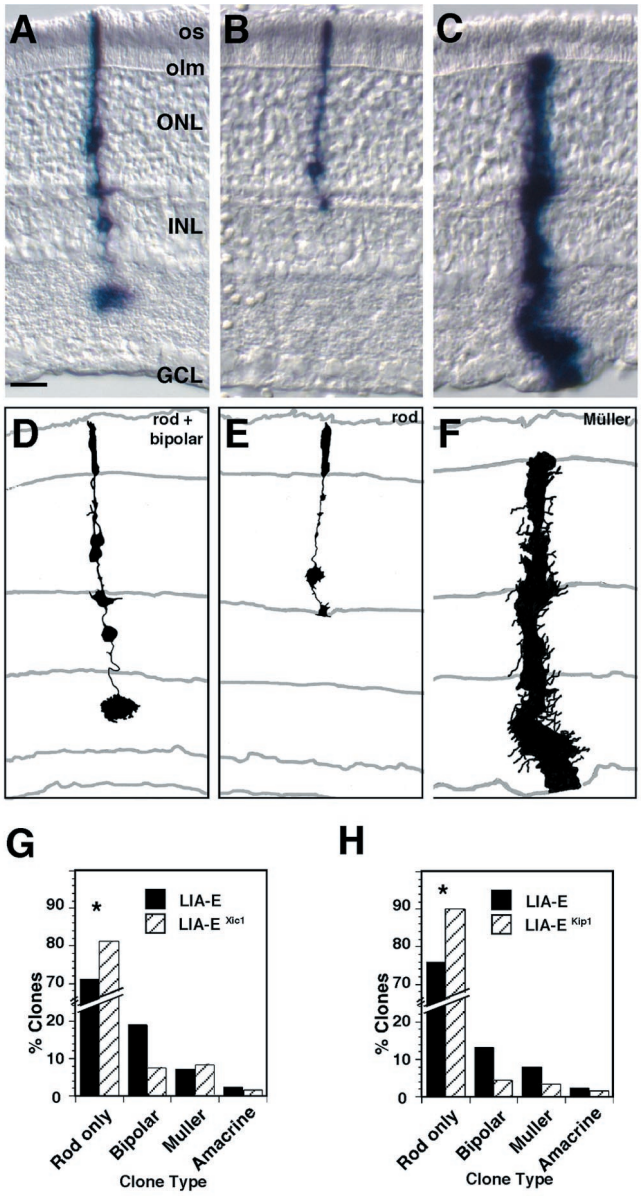

Figure 4. Overexpression of p27^{Kip1} and p27^{Xic1} *in vivo* using replication incompetent retroviral vectors. *In vivo* lineage analysis was performed by injecting LIA-E and LIA-E^{Kip1} or LIA-E and LIA-E^{Xic1} into the eyes of newborn rat pups. Photos (*A–C*) and (*D–F*) drawings of representative clone types from lineage studies are shown. Clones containing bipolar cells (*A*, *D*), rods (*B*, *E*), Müller glia (*C*, *F*), and amacrine cells (data not shown) can be identified readily by morphology and position within the laminar structure of the retina. Data presented in *G* are from multiple retinas from two independent litters and represent 416 clones for LIA-E^{Xic1} and 165 clones for LIA-E. Data presented in *H* are from 176 clones for pLIA-E^{Kip1} and 294 clones for pLIA-E. *Asterisk* indicates that an increase in the proportion of single-rod clones (81% for LIA-E^{Xic1} and 47% for LIA-E; 82% for LIA-E^{Kip1} and 63% for LIA-E) was seen among the rod-only clones. *os*, Photoreceptor outer segment; *olm*, outer limiting membrane; *ONL*, outer nuclear layer; *INL*, inner nuclear layer; *GCL*, ganglion cell layer. Scale bar, 10 μm.

tion of bipolar cells was decreased from 9.4% (32/337) for LIA-E to 6.2% (35/563) for LIA-E^{Xic1}. However, the proportion of clones containing Müller glia was only slightly increased from 8% (14/165) for LIA-E to 10% (43/416) for LIA-E^{Xic1} (Fig. 4*G*). This difference is more pronounced when the proportion of cells is compared [4.1% (14/337) for LIA-E to 7.6% (43/563) for LIA-E^{Xic1}] rather than the proportion of clones containing those cells. Furthermore, mitotic retinal progenitor cells prematurely exited the cell cycle as indicated by an increase in the proportion of single rod clones among the clones that contain only rods (47% for LIA-E and 81% for LIA-E^{Xic1}).

To determine whether overexpression of the mouse p27^{Kip1} was sufficient to force retinal progenitor cells out of the cell cycle *in vivo* and whether Müller glial/bipolar cell fate specification was perturbed, we performed a similar lineage study with LIA-E^{Kip1}. The titer of the LIA-E^{Kip1} retrovirus was significantly lower on 3T3 cells ($\sim 1 \times 10^{-6}$/ml) than that obtained for LIA-E^{Xic1} ($\sim 5 \times 10^{-6}$/ml). This disparity in titer was also reflected in the average number of clones per retina (~12 clones per retina for LIA-E^{Kip1} and ~50 clones per retina for LIA-E^{Xic1}) for the *in vivo* lineage analysis. Although we could not detect any cytotoxicity/apoptosis as a result of p27^{Kip1} misexpression (Fig. 3, and see above), it is possible that a subset of cells was selectively killed as a result of persistent p27^{Kip1} expression. Low titer notwithstanding, there was an obvious reduction in the size of clones derived from progenitor cells infected with LIA-E^{Kip1} (82% of rod-only clones were single-rod clones as compared with 63% for LIA-E). As expected (see Discussion), on the basis of this premature cell cycle exit, there was a slight reduction in the percentage of clones containing Müller glial cells as well as clones containing bipolar cells (Fig. 4*H*). The proportion of Müller glial cells among all the infected cells was similarly reduced from 5.3% (24/446) for LIA-E to 2.7% (8/388) for LIA-E^{Kip1}. Bipolar cells were reduced from 8.7% (39/446) for LIA-E to 5.5% (16/388) for LIA-E^{Kip1}.

Cell cycle exit in the p27^{Kip1}-deficient retinas

Mice carrying a targeted disruption of the p27^{Kip1} gene have been described previously and were found to exhibit multiple organ hyperplasia and increased body size as a result of increased proliferation (Fero et al., 1996; Kiyokawa et al., 1996; Nakayama et al., 1996). To test whether retinal progenitor cells undergo additional rounds of cell division in the absence of p27^{Kip1}, a BrdU pulse-labeling experiment was performed (Fig. 5*A*,*B*). At least 500 cells were scored from 8–12 retinas from five stages of development and in adult retinas (Fig. 5*C*) (data not shown). After scoring, genotypes were determined, and the data from the wild-type, p27^{Kip1} heterozygous, or p27^{Kip1}-deficient animals were averaged (Fig. 5*C*). The proportion of mitotic cells observed at E14.5 in the p27^{Kip1}-deficient retinas was significantly higher (40 ± 2.8%) than that of their wild-type littermates (26 ± 5.1%; $p < 0.007$) (Fig. 5*C*). The proportion of mitotic cells in retinas from p27$^{Kip1+/-}$ animals (32 ± 1.7%) was intermediate between the data for the wild-type and knock-out mice (Fig. 5*C*). At E16.5, P0, P3, and P10, a similar pattern was observed (Fig. 5*C*). No mitotic cells were observed in retinas from adult animals at 3 weeks or 3 months of age for the p27^{Kip1}-deficient or p27^{Kip1}-heterozygous mice (data not shown).

Apoptosis in the retinas from p27$^{-/-}$ and p27$^{+/-}$ mice

As with the p27^{Kip1}-deficient retinas, an increase in the proportion of mitotic cells was observed in the retinas from p57^{Kip2} knock-out mice (Dyer and Cepko, 2000a). This increased proliferation was accompanied by an increase in apoptosis during the stage when p57^{Kip2} was normally expressed and compensated for the extra cells in the p57^{Kip2} knock-out retina. To test whether a similar compensation mechanism was occurring in the p27^{Kip1}-deficient or p27^{Kip1}-heterozygous retinas, a TUNEL assay was

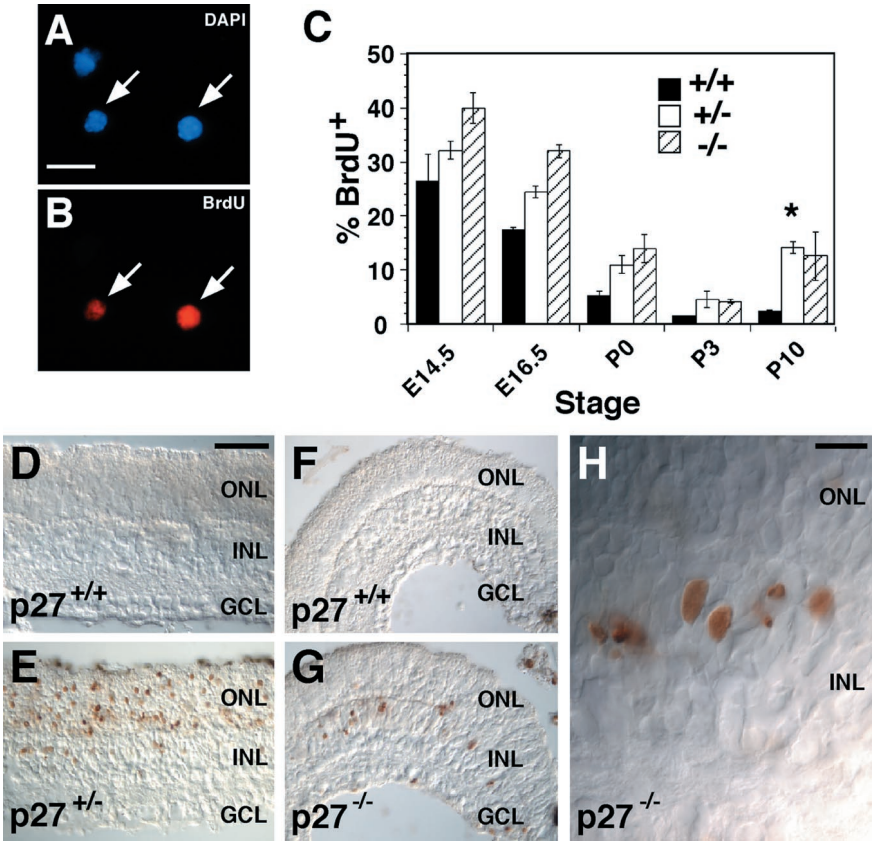

Figure 5. BrdU and TUNEL labeling of $p27^{Kip1}$-deficient retinas. The proportion of mitotic cells in wild type, $p27^{Kip1+/-}$, and $p27^{Kip1-/-}$ retinas was assayed by performing BrdU labeling at five different stages of development. *A*, *B*, E14.5 retinal progenitor cells in S-phase at the time of labeling were detected by anti-BrdU immunofluorescence (*arrows*). Scale bar, 10 μm. *C*, The proportion of BrdU-positive retinal cells after a 1 or 4 hr (*asterisk*) incubation. Each *bar* represents the average of 500 cells scored for two to four independent retinas. Apoptosis was monitored in wild-type, $p27^{Kip1+/-}$, and $p27^{Kip1-/-}$ retinas at the five stages of development examined in *C*. *D*, *E*, Apoptotic nuclei in the central retina from wild-type (*D*) and $p27^{Kip1}$-heterozygous mice (*E*) at P10.5. *F*, *G*, Apoptotic nuclei in the peripheral retina from wild-type (*F*) and $p27^{Kip1}$-deficient mice (*G*) at P10.5. *H*, An enlarged view showing clear apoptotic nuclei in the center of the INL in a $p27^{Kip1}$-deficient retina. Scale bar: *D–G*, 100 μm; *H*, 10 μm. *ONL*, Outer nuclear layer; *INL*, inner nuclear layer; *GCL*, ganglion cell layer.

performed on retinas from each stage of development examined above for BrdU labeling. During the early stages of development (E14.5 and E16.5), very few apoptotic nuclei were observed in any of the animals (data not shown). However, as development progressed the presence of an increased proportion of apoptotic nuclei was apparent in the $p27^{Kip1-/-}$ and $p27^{Kip1+/-}$ retinas as compared with their wild-type littermates. This difference was most significant at P10.5 (Fig. 5*D–H*). The proportion of apoptotic nuclei appeared to be greater in the $p27^{Kip1+/-}$ retinas than the $p27^{Kip1-/-}$ retinas, particularly in the outer nuclear layer (Fig. 5*E*).

Quantitation of the major retinal cell types in the $p27^{+/-}$ and $p27^{-/-}$ mice

To test whether the additional proliferation and apoptosis of the $p27^{Kip1}$ mutant retina resulted in aberrant production or survival of particular cell types, the proportion of several classes of retinal cell types was examined in adult retinas from wild-type, $p27^{Kip1+/-}$ and $p27^{Kip1-/-}$ mice. Retinas from 6-week-old mice from a cross of $p27^{+/-}$ parents were dispersed, plated, and stained with various cell type-specific antibodies (Fig. 6*A–E*). Mice were genotyped after cell counting, and data from each genotype were pooled to obtain the mean and SD for each group of samples (Fig. 6*F*). Rod photoreceptors (Fig. 6*A*) constitute the majority of cells in the adult murine retina, and no significant difference in the proportion of rhodopsin-immunoreactive photoreceptors was found in mice lacking one or both alleles of $p27^{Kip1}$ (Fig. 6*F*). The proportion of Müller glial cells, as measured by CRALBP immunoreactivity (Fig. 6*E*), was not decreased in the retinas from mice deficient for $p27^{Kip1}$ (Fig. 6*F*). We did find, however, a dramatic (10- to 20-fold) increase in the proportion of Müller glial cells expressing glial fibrillary acidic protein, which is an intermediate filament protein found in Müller cells undergoing reactive gliosis (Dyer and Cepko, 2000b). The other major retinal cell types, 115A10 and Chx10 immunoreactive bipolar cells (Fig. 6*D*) (data not shown), syntaxin immunoreactive amacrine cells (Fig. 6*C*), and calbindin immunoreactive horizontal cells (Fig. 6*B*) were present in approximately the same proportion in the retinas from all of the mice examined (Fig. 6*F*). Furthermore, amacrine cell subpopulations (calretinin, calbindin, ChAT, parvalbumin, and $p57^{Kip2}$) were unaffected in the retinas from mice lacking one or both alleles of $p27^{Kip1}$ (data not shown).

Organization of cell types in the $p27^{Kip1}$-deficient retinas

To determine whether the major retinal cell types were organized appropriately into the correct laminas of the retinas in the $p27^{Kip1}$-deficient mice, immunohistochemical staining was performed on retinal sections using the same antibodies described above. We found that the boundaries between the cellular layers of the retina in the $p27^{Kip1}$-deficient mice were disrupted. The cell bodies of the rhodopsin-immunoreactive photoreceptors were found outside the outer limiting membrane, and the photoreceptor outer segments were often missing in those regions (Fig. 7*A*,*B*). The photoreceptor layer of the $p27^{+/-}$ retinas did not exhibit the type of retinal dysplasia (Nakayama et al., 1996) seen in the $p27^{-/-}$ retinas. However, the boundaries between the outer nuclear layer and the inner nuclear layer did not appear as regular as in the wild-type littermates (data not shown). Additionally, bipolar interneurons (Fig. 7*C*,*D*) and horizontal cells (Fig. 7*E–H*) were displaced from their normal positions in the INL. Amacrine cells (data not shown) and amacrine cell subpopulations [calbindin (Fig. 7*G*,*H*); calretinin (Fig. 7*I*,*J*); $p57^{Kip2}$

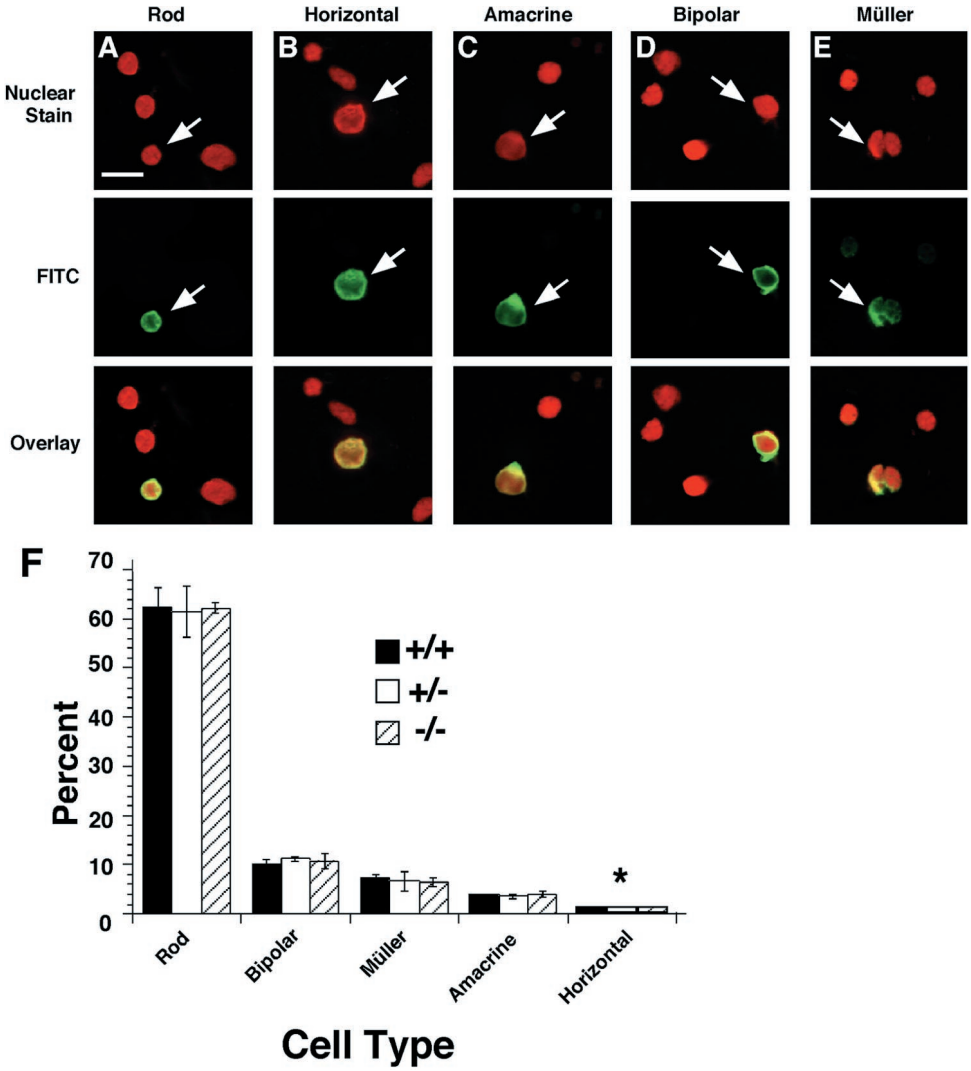

Figure 6. Quantitation of the major cell types in the $p27^{Kip1}$-deficient retinas. Dissociated adult retinas from $p27^{Kip1+/+}$, $p27^{Kip1+/-}$, and $p27^{Kip1-/-}$ mice were stained with cell type-specific antibodies. *A–E*, Representative examples of dissociated retinal cell types. *A*, Rhodopsin-immunoreactive rod photoreceptor; *B*, calbindin-immunoreactive horizontal cell; *C*, syntaxin-1-immunoreactive amacrine cell; *D*, 115A10-immunopositive bipolar cell; *E*, CRALBP- immunoreactive Müller glial cell. *F*, The proportion of immunoreactive cells for each antibody shown in *A–E* was determined for several mice from independent litters for each genotype indicated. For rods and bipolars, each *bar* represents the average of 500 cells scored from each retina; for Müller glial cells and amacrine cells, each *bar* represents the average of 1000 cells scored from each retina; and for horizontal cells, each *bar* represents the average of 2500 cells scored for each retina. Scale bar, 10 μm.

(Fig. 7*K*,*L*)] appeared to be localized to the correct region of the INL, yet their overall organization was not as regular as that seen in the wild-type retinas.

DISCUSSION

We have presented several lines of evidence to suggest that $p27^{Kip1}$ is an important regulator of retinal progenitor cell proliferation during development. $p27^{Kip1}$ was found to be upregulated during the late G_2 or early G_1 phase of the cell cycle, overexpression of $p27^{Kip1}$ in mitotic retinal progenitor cells led to premature cell cycle exit, and an increase in the proportion of mitotic cells was observed in the retinas from mice lacking one or both alleles of $p27^{Kip1}$. Surprisingly, the proportion of the major retinal cell types in the mature retinas from $p27^{Kip1}$-deficient mice was normal, suggesting that there was compensation for the extra rounds of cell division. In fact, more apoptosis was found in the $p27^{Kip1-/-}$ retinas, most likely accounting, at least in part, for this compensation. Overexpression of $p27^{Kip1}$ using transduction via a retrovirus vector *in vivo* and *in vitro* led to smaller clones, suggesting that $p27^{Kip1}$ is not only required for proper exit from the cell cycle but is sufficient to induce it. However, in contrast to the *Xenopus* $p27^{Xic1}$ cyclin kinase inhibitor, mouse $p27^{Kip1}$ did not lead to any obvious perturbation in cell fate determination that could not be explained by the premature cell cycle exit of retinal progenitor cells. Significantly, $p27^{Kip1}$ and $p57^{Kip2}$, two regulators of cell cycle exit of the Cip/Kip family, were expressed in distinct retinal progenitor cell populations and upregulated at different times in the cell cycle.

Retinal progenitor cells use at least two different cyclin kinase inhibitors to exit the cell cycle

Previous work has demonstrated that the $p57^{Kip2}$ cyclin kinase inhibitor mediates cell cycle exit in a restricted subset (~16%) of embryonic retinal progenitor cells (Dyer and Cepko, 2000a). We have shown here that the $p27^{Kip1}$ cyclin kinase inhibitor is expressed in a distinct population of retinal progenitor cells during embryonic development. Not only were these two proteins expressed in different groups of progenitor cells, they were upregulated during different phases of the cell cycle. $p27^{Kip1}$ expression was detected within 8 hr of S-phase at E14.5, which is consistent with the late G_2 or early G_1 phase of the cell cycle. Because the length of the cell cycle increased during development (Alexiades and Cepko, 1996), the timing of $p27^{Kip1}$ upregulation after S-phase was similarly delayed. This may indicate that upregulation of $p27^{Kip1}$ in retinal progenitor cells occurs at the same phase of the cell cycle regardless of cell cycle length. In contrast to the timing of $p27^{Kip1}$ upregulation, $p57^{Kip2}$ expression was not detected until 16 hr after S-phase, which is consistent with ex-

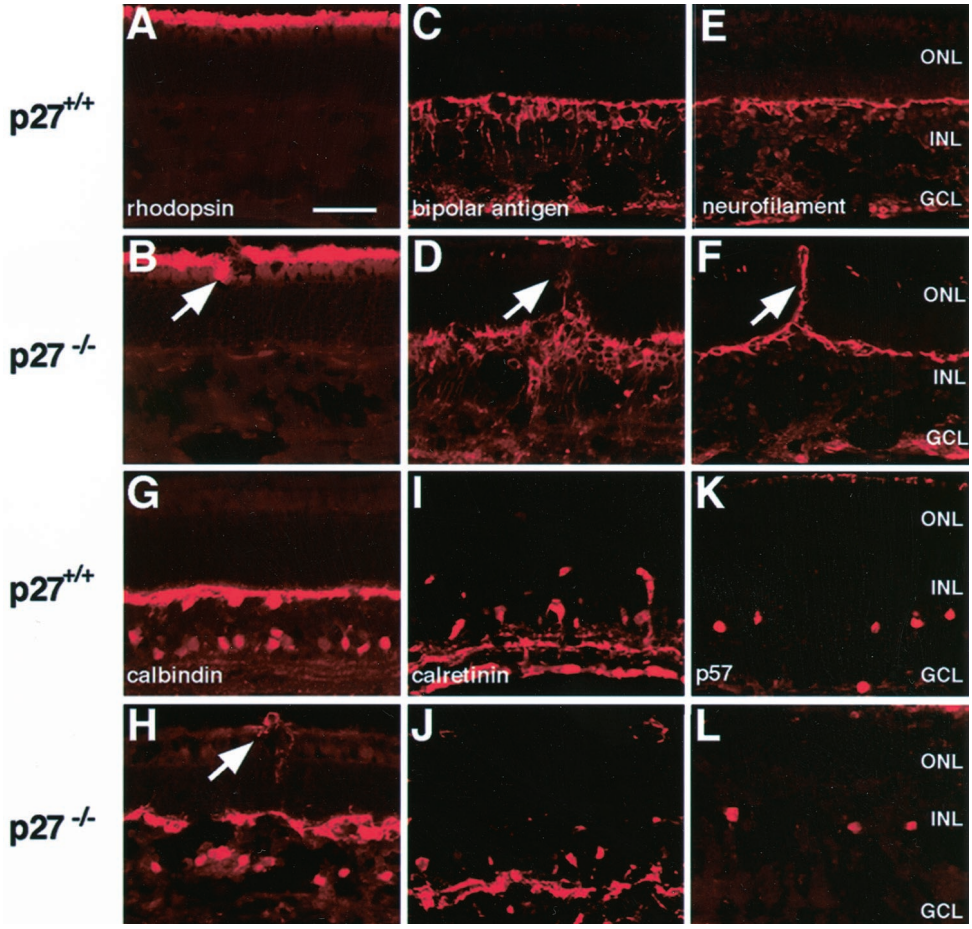

Figure 7. Distribution of the major cell types in the $p27^{Kip1}$-deficient retinas. Retinal cryosections from wild-type and $p27^{Kip1-/-}$ mice were stained with cell type-specific antibodies. Dysplastic lesions in the $p27^{Kip1}$-deficient retinas are indicated by *arrows*. *A*, *B*, Wild-type and $p27^{Kip1}$-deficient retinas stained with the anti-rhodopsin antibody (Rho4D2). *C*, *D*, Bipolar interneurons were detected using the 115A10 monoclonal antibody. *E–H*, Neurofilament- and calbindin-immunoreactive horizontal cells. Immunohistochemical staining of an amacrine cell subpopulation using an antibody directed against calretinin (*I*, *J*) and a distinct population that expresses $p57^{Kip2}$ (*K*, *L*). Scale bar, 100 μm. *ONL*, Outer nuclear layer; *INL*, inner nuclear layer; *GCL*, ganglion cell layer.

pression in the late G_1 or G_0 phase of the cell cycle (Dyer and Cepko, 2000a).This is the first example of retinal progenitor heterogeneity with respect to the mechanism of cell cycle exit. For example, progenitor cells may have the ability to produce different daughter cell types because of the usage of different cyclin kinase inhibitors ($p27^{Kip1}$ vs $p57^{Kip2}$) (Alexiades and Cepko, 1997; Dyer and Cepko, 2000a). Alternatively, work on *Dictyostelium* has demonstrated that cells respond differently to the same stimuli depending on cell cycle phase (Gomer and Ammann, 1996). Thus, the time within the cell cycle that a retinal progenitor cell decides to produce a postmitotic daughter cell, or to become postmitotic, may influence which cyclin kinase inhibitor is upregulated. For example, if a progenitor cell decides to produce a postmitotic daughter between the late G_2 and early G_1 phases of the cell cycle, then $p27^{Kip1}$ might be upregulated, whereas if the decision to exit the cell cycle is delayed by several hours (late G_1 phase), a progenitor cell might upregulate $p57^{Kip2}$. Because changes in the competence of retinal progenitor cells to produce different retinal cell types occurs during retinal development concomitant with changes in the kinetics of cell cycle and mitotic fate of daughter cells, it is possible that all of these changes are linked.

In retinas from $p27^{Kip1}$-deficient mice, the proportion of mitotic cells was increased in comparison to their wild-type littermates. However, this difference was somewhat lower than expected considering the broad expression of $p27^{Kip1}$ during development. Thus, in the absence of $p27^{Kip1}$, retinal progenitor cells may use an alternative, semi-redundant mechanism to exit the cell cycle. The most obvious possibility would be the presence of one or more additional cyclin kinase inhibitors. Consistent with this model, we have found that in addition to $p27^{Kip1}$ and $p57^{Kip2}$, there are two other cyclin kinase inhibitors expressed in the developing mouse retina (our unpublished observations). It is also possible that in the absence of $p27^{Kip1}$, proteins that do not normally act as cyclin kinase inhibitors may serve that role. Specifically, work on mouse embryonic fibroblasts lacking $p27^{Kip1}$ demonstrated that a member of the retinoblastoma (Rb) family of proteins can serve as a cyclin kinase inhibitor in those cells (Zhu et al., 1995; Woo et al., 1997; Coats et al., 1999). All three Rb family members are expressed in the murine retina (our unpublished observations), and one or more of these molecules may mediate cell cycle exit in the absence of $p27^{Kip1}$. Finally, our expression studies revealed that cyclin D1 is rapidly downregulated in newly postmitotic daughter cells. Therefore, the precise timing of cell cycle exit may be a two-step process: downregulation of cyclin D1 and upregulation of a cyclin kinase inhibitor. In the absence of $p27^{Kip1}$, progenitor cells may still eventually exit the cell cycle simply through their normal process of downregulating cyclin D1.

Extra cells in the $p27^{Kip1}$-deficient retinas are eliminated by apoptosis during the late perinatal stages of development

Because of the birth order of retinal cell types during development, perturbations in progenitor cell proliferation could affect the proportion of one or more of these cell types in the mature

tissue. The increase in mitoses observed throughout development in the $p27^{Kip1}$-deficient retina could lead to a large cumulative change in retinal cell number such that a change in the proportions of retinal cell types might have been observed in the adult. Surprisingly, there was no change in the proportions of retinal neurons or glia in the adult retina. Previous work on the $p57^{Kip2}$-deficient retina demonstrated that inappropriate S-phase entry was quickly followed by apoptosis during the embryonic period when $p57^{Kip2}$ is expressed (Dyer and Cepko, 2000a). However, very little apoptosis was detected throughout much of development in the $p27^{Kip1}$-deficient retina, although there was a greater than normal proportion of cells in S-phase. In contrast to our observations of the timing of apoptosis in the $p57^{Kip2}$ deficient retinas, an enormous number of apoptotic nuclei were observed in the retinas from mice lacking one or both alleles of $p27^{Kip1}$ after proliferation was complete (P10.5). This may indicate that the extra cells generated during retinal development were not eliminated when they reentered the cell cycle, as seen in the $p57^{Kip2}$-deficient retina, but were eliminated all at once postnatally.

This difference in the timing of apoptosis in $p27^{Kip1}$- and $p57^{Kip2}$-deficient retinas may indicate that the two genes play different roles. $p57^{Kip2}$ may be required to prevent reentry of cells into S-phase after they have entered G_0. The observation that $p57^{Kip2}$-deficient cells undergo apoptosis after they have migrated to the inner retina (Dyer and Cepko, 2000a) where they most likely would be beginning to differentiate as amacrine cells supports the notion that they are attempting to enter S-phase from G_0. This type of behavior apparently leads to immediate apoptosis, not only in the $p57^{Kip2}$-deficient retinas, but also in the CNS of Rb-deficient mice (Lee et al., 1992). The role played by $p57^{Kip2}$ thus seems distinct from that of $p27^{Kip1}$ in terms of two criteria: (1) kinetics of synthesis during the cell cycle (late G_1/G_0 for $p57^{Kip2}$ and late G_2/early G_1 for $p27^{Kip1}$ and (2) timing of apoptosis (immediate for $p57^{Kip2}$-deficient retinas and delayed for $p27^{Kip1}$-retinas). The delay in apoptosis for $p27^{Kip1}$-deficient retinas suggests that these cells simply fail to exit the cell cycle and continue to proliferate somewhat normally, as opposed to reentering the cell cycle from an inappropriate stage of the cell cycle or using an aberrant mechanism. The extra cells that are generated in the $p27^{Kip1}$-deficient retinas are therefore "normal" but in excess. The excess is then partially or completely eliminated at the end of development.

Despite the normal proportion of retinal cell types in mice lacking one or both alleles of $p27^{Kip1}$, we found that the organization of these cell types was perturbed. These defects occurred in regions of retinal dysplasia described previously (Nakayama et al., 1996). We have since found that retinal dysplasia results from reactive gliosis involving Müller glial cells during development (Dyer and Cepko, 2000b). That is, disruptions in the outer limiting membrane, which is made up of Müller cell apical microvilli, probably result in the retinal disorganization described here. Furthermore, vascular defects seen in the retinas from $p27^{Kip1}$-deficient mice (Dyer and Cepko, 2000b) may also be a contributing factor.

$p27^{Kip1}$ does not play a direct role in cell fate specification or differentiation in the murine retina

Significant evidence is accumulating that cyclin kinase inhibitors can influence developmental processes beyond their prescribed role in proliferation control (Zhang et al., 1997; Ohnuma et al., 1999; Dyer and Cepko, 2000a). In the *Xenopus* retina, overexpression of $p27^{Xic1}$ led to an increase in the proportion of Müller glial cells and a reduction in the proportion of bipolar cells (Ohnuma et al., 1999). When $p27^{Xic1}$ expression was blocked, a decrease in Müller glial cells was observed along with an increase in bipolar interneurons. We found that overexpression of $p27^{Xic1}$ in murine retinal progenitor cells *in vivo* led to a reduction in clone size and a decrease in the proportion of clones containing bipolar cells and a modest increase in the proportion of clones containing Müller glia. However, when the total population of cells infected was considered rather than the clonal composition, there was a decrease in bipolar cells from 9.4% (32/337) for LIA-E to 6.2% (35/563) for LIA-E^{Xic1} and an increase in the Müller glial cells from 4.1% (14/337) for LIA-E to 7.6% (43/563) for LIA-E^{Xic1}. These approximately twofold differences are similar to the data obtained in *Xenopus* for the total population of transduced cells at a similar stage of development (stage 21–24) (Ohnuma et al., 1999). Therefore, our data indicate that $p27^{Xic1}$ has a similar affect on rodent retinal progenitor cell proliferation and specification/differentiation as was shown previously for *Xenopus* retinal progenitor cells (Ohnuma et al., 1999).

The murine cyclin kinase inhibitor, $p27^{Kip1}$, also led to a reduction in clone size and a reduction in the proportion of clones containing bipolar cells. However, in contrast to the *Xenopus* Xic1 protein, mouse $p27^{Kip1}$ did not increase the proportion of clones containing Müller glial cells but actually decreased them slightly. Considering that Müller glial cells and bipolar cells are among the last cell types to be generated during retinal histogenesis, premature cell cycle exit should reduce the proportion of clones containing those cell types. Furthermore, the peak period of rod photoreceptor genesis occurs just before the peaks for bipolar and Müller glial cells. Thus, it is not surprising that premature cell cycle exit mediated by $p27^{Kip1}$ would lead to an increase in the proportion of clones containing rod photoreceptors, as we observed. Indeed, misexpression of other cyclin kinase inhibitors in the developing rodent retina has also led to a reduction in bipolar and Müller glial cells accompanied by an increase in the proportion of clones containing rod photoreceptors (our unpublished observations). These data, combined with the aforementioned observation that the knock-out retinas had no major defect in the proportion of any of the retinal cell types, suggest that $p27^{Kip1}$ is not likely to play a direct role in cell fate specification in the murine retina.

There are several possible models for the role of p27 in retinal development that can explain the differences between Xic1 and Kip1 after misexpression in the *Xenopus* and murine retina. At the moment, it is not clear which model is correct. When overexpressed in the rodent retina, $p27^{Kip1}$ and $p27^{Xic1}$ gave different results regarding the number of Müller glia, suggesting that the two proteins are different with respect to their ability to induce this cell type. In contrast, in *Xenopus*, both proteins increased the number of Müller glia, which would suggest that they are similar in their ability to induce this cell type. When one examines the loss of function data, it is supportive of the overexpression data in each organism. Loss of function in the murine retina had no obvious effect on cell fate specification, whereas a reduction in the expression of $p27^{Xic1}$ in the *Xenopus* retina did affect cell fate specification. Because Xic1 does not appear to have an ortholog in mammals and shares distinct sequence homology regions with different members of the mammalian Cip/Kip family (Ohnuma et al. 1999), it could be that the two proteins play different roles in their respective organisms. This may part be explained in part by the rapidity with which the *Xenopus* retina is built, relative to the murine retina. In *Xenopus*, nearly half of the total number of cells,

representing all of the major cell types, are produced in the amount of time it takes to progress through one round of cell division in mice (~10 hr). In mice, retinal histogenesis takes well over 2 weeks (Young, 1985), which is equivalent to ~8–10 rounds of cell division (Alexiades and Cepko, 1996). Thus, the regulation of proliferation, the consequences of altered proliferation, and any changes in progenitor cell competence to make different cell types might be different in the different organisms.

Cyclin kinase inhibitors play multiple, distinct roles in the formation and maintenance of a healthy retina

We have recently learned a great deal about the roles that cyclin kinase inhibitors can play in the vertebrate retina. It was not surprising to find, as we have shown here, that cyclin kinase inhibitors regulate progenitor cell proliferation during retinal development (Ohnuma et al., 1999; Dyer and Cepko, 2000a). However, the evidence for progenitor cell heterogeneity in terms of cell cycle exit ($p27^{Kip1}$ vs $p57^{Kip2}$ and possibly cyclin D1 vs cyclin D3) was unexpected and important for our understanding of retinal development. Beyond proliferation control, cyclin kinase inhibitors can also regulate cell fate specification and differentiation in the retina (Ohnuma et al., 1999; Dyer and Cepko, 2000a). In addition to these developmental processes, recent findings have shown that a cyclin kinase inhibitor ($p27^{Kip1}$) is important for the initial response to injury in the adult retina (Dyer and Cepko, 2000b). Significantly, downregulation of $p27^{Kip1}$ is the earliest molecular event identified to date characteristic of Müller glial cells undergoing reactive gliosis. When taken together, these related studies and the data presented here indicate that cyclin kinase inhibitors can play diverse and often unexpected roles in the developing and mature vertebrate retina.

REFERENCES

Alexiades MR, Cepko C (1996) Quantitative analysis of proliferation and cell cycle length during development of the rat retina. Dev Dyn 205:293–307.

Alexiades MR, Cepko CL (1997) Subsets of retinal progenitors display temporally regulated and distinct biases in the fates of their progeny. Development 124:1119–1131.

Belliveau MJ, Cepko CL (1999) Extrinsic and intrinsic factors control the genesis of amacrine and cone cells in the rat retina. Development 126:555–566.

Belliveau MJ, Young TL, Cepko CL (2000) Late retinal progenitor cells show intrinsic limitations in the production of cell types and the kinetics of opsin synthesis. J Neurosci 20:2247–2254.

Bobrow MN, Shaughnessy KJ, Litt GJ (1991) Catalyzed reporter deposition, a novel method of signal amplification. II. Application to membrane immunoassays. J Immunol Methods 137:103–112.

Cepko CL, Austin CP, Yang X, Alexiades M, Ezzeddine D (1996) Cell fate determination in the vertebrate retina. Proc Natl Acad Sci USA 93:589–595.

Cepko CL, Fields-Berry S, Ryder E, Austin C, Golden J (1998) Lineage analysis using retroviral vectors. Curr Top Dev Biol 36:51–74.

Chiu MI, Zack DJ, Wang Y, Nathans J (1994) Murine and bovine blue cone pigment genes: cloning and characterization of two new members of the S family of visual pigments. Genomics 21:440–443.

Chomczynski P, Sacchi N (1987) Single-step method of RNA isolation by acid guanidinium thiocyanate-phenol-chloroform extraction. Anal Biochem 162:156–159.

Coats S, Whyte P, Fero ML, Lacy S, Chung G, Randel E, Firpo E, Roberts JM (1999) A new pathway for mitogen-dependent cdk2 regulation uncovered in p27(Kip1)-deficient cells. Curr Biol 9:163–173.

De Leeuw AM, Gaur VP, Saari JC, Milam AH (1990) Immunolocalization of cellular retinol-, retinaldehyde- and retinoic acid-binding proteins in rat retina during pre- and postnatal development. J Neurocytol 19:253–264.

Dyer MA, Cepko CL (2000a) p57 regulates progenitor cell proliferation and amacrine interneuron development in the mouse retina. Development 127:3593–3605.

Dyer MA, Cepko CL (2000b) Control of Müller glial cell proliferation and activation following retinal injury. Nat Neurosci 3:873–880.

Dyer MA, Cepko CL (2001) The $p57^{Kip2}$ cyclin kinase inhibitor is expressed by a restricted set of amacrine cells in the rodent retina. J Comp Neurol 429:601–614.

Fantl V, Stamp G, Andrews A, Rosewell I, Dickson C (1995) Mice lacking cyclin D1 are small and show defects in eye and mammary gland development. Genes Dev 9:2364–2372.

Farrington SM, Belaoussoff M, Baron MH (1997) Winged-helix, Hedgehog and Bmp genes are differentially expressed in distinct cell layers of the murine yolk sac. Mech Dev 62:197–211.

Fero ML, Rivkin, M, Tasch, M, Porter, P, Carow CE, Firpo, E, Polyak, K, Tsai LH, Broudy, V, Perlmutter RM, Kaushansky, K, Roberts JM (1996) A syndrome of multiorgan hyperplasia with features of gigantism, tumorigenesis, and female sterility in p27(Kip1)-deficient mice. Cell 85:733–744.

Fields-Berry SC, Halliday AL, Cepko CL (1992) A recombinant retrovirus encoding alkaline phosphatase confirms clonal boundary assignment in lineage analysis of murine retina. Proc Natl Acad Sci USA 89:693–697.

Gomer RH, Ammann RR (1996) A cell-cycle phase-associated cell-type choice mechanism monitors the cell cycle rather than using an independent timer. Dev Biol 174:82–91.

Holt CE, Bertsch TW, Ellis HM, Harris WA (1988) Cellular determination in the *Xenopus* retina is independent of lineage and birth date. Neuron 1:15–26.

Kiyokawa H, Kineman RD, Manova-Todorova KO, Soares VC, Hoffman ES, Ono M, Khanam D, Hayday AC, Frohman LA, Koff A (1996) Enhanced growth of mice lacking the cyclin-dependent kinase inhibitor function of p27(Kip1). Cell 85:721–732.

Lee E, Chang C, Nanpin H, Wang YJ, Lai C, Herrup K, Lee W, Bradley A (1992) Mice deficient for Rb are nonviable and show defects in neurogenesis and haematopoiesis. Nature 359:288–294.

Levine EM, Close J, Fero M, Ostrovsky A, Reh TA (2000) p27(Kip1) regulates cell cycle withdrawal of late multipotent progenitor cells in the mammalian retina. Dev Biol 219:299–314.

Ma C, Papermaster D, Cepko CL (1998) A unique pattern of photoreceptor degeneration in cyclin D1 mutant mice. Proc Natl Acad Sci USA 95:9938–9943.

Molday RS, MacKenzie D (1983) Monoclonal antibodies to rhodopsin: characterization, cross-reactivity, and application as structural probes. Biochemistry 22:653–660.

Morrow EM, Belliveau MJ, Cepko CL (1998) Two phases of rod photoreceptor differentiation during rat retinal development. J Neurosci 18:3738–3748.

Nakayama K, Ishida N, Shirane M, Inomata A, Inoue T, Shishido N, Horii I, Loh DY (1996) Mice lacking p27(Kip1) display increased body size, multiple organ hyperplasia, retinal dysplasia, and pituitary tumors. Cell 85:707–720.

Ohnuma S, Philpott A, Wang K, Holt CE, Harris WA (1999) p27Xic1, a Cdk inhibitor, promotes the determination of glial cells in *Xenopus* retina. Cell 99:499–510.

Onoda N, Fujita SC (1987) A monoclonal antibody specific for a subpopulation of retinal bipolar cells in the frog and other vertebrates. Brain Res 416:359–363.

Rodieck RW (1998) The first steps in seeing. Sunderland, MA: Sinauer.

Sanchez I, Dynlacht BD (1996) Transcriptional control of the cell cycle. Curr Opin Cell Biol 8:318–324.

Sauer FC (1937) The interkinetic migration of embryonic epithelial nuclei. J Morphol 61:553–579.

Sicinski P, Donaher JL, Parker SB, Li T, Fazeli A, Gardner H, Haslam SZ, Bronson RT, Elledge SJ, Weinberg RA (1995) Cyclin D1 provides a link between development and oncogenesis in the retina and breast. Cell 82:621–630.

Turner DL, Cepko CL (1987) A common progenitor for neurons and glia persists in rat retina late in development. Nature 328:131–136.

Turner DL, Snyder EY, Cepko CL (1990) Lineage-independent determination of cell type in the embryonic mouse retina. Neuron 4:833–845.

Wang SZ, Adler R, Nathans J (1992) A visual pigment from chicken that resembles rhodopsin: amino acid sequence, gene structure, and functional expression. Biochemistry 31:3309–3315.

Woo MS, Sanchez I, Dynlacht BD (1997) p130 and p107 use a conserved domain to inhibit cellular cyclin-dependent kinase activity. Mol Cell Biol 17:3566–3579.

Young RW (1985) Cell differentiation in the retina of the mouse. Anat Rec 212:199–205.

Zhang P, Liegeois NJ, Wong C, Finegold M, Hou H, Thompson JC, Silverman A, Harper JW, DePinho RA, Elledge SJ (1997) Altered cell differentiation and proliferation in mice lacking p57KIP2 indicates a role in Beckwith-Wiedemann syndrome. Nature 387:151–158.

Zhang P, Wong C, DePinho RA, Harper JW, Elledge SJ (1998) Cooperation between the Cdk inhibitors p27(KIP1) and p57(KIP2) in the control of tissue growth and development. Genes Dev 12:3162–3167.

Zhu L, Harlow E, Dynlacht BD (1995) p107 uses a p21CIP1-related domain to bind cyclin/cdk2 and regulate interactions with E2F. Genes Dev 9:1740–1752.